Journal of Pharmacological and Toxicological Methods 124 (2023) 107480

Contents lists available at ScienceDirect

Journal of Pharmacological and Toxicological Methods

journal homepage: www.elsevier.com/locate/jpharmtox

Telemetric long-term assessment of autonomic function in experimental heart failure

Katharina Boden [a,b], Pailin Pongratanakul [a,c], Julia Vogel [b,d], Nicola Willemsen [a,e], Eva-Maria Jülke [f], Jakob Balitzki [a,h], Hanna Tinel [a], Hubert Truebel [b], Wilfried Dinh [a,b,g], Thomas Mondritzki [a,b,*]

[a] Bayer AG, Wuppertal, Germany
[b] University of Witten/Herdecke, Witten, Germany
[c] University of Cologne, Germany
[d] Clinic for Cardiology and Angiology, West-German Heart and Vascular Center, Faculty of Medicine, University Duisburg-Essen, Germany
[e] University of Duisburg-, Essen, Germany
[f] Leipzig University, Leipzig, Germany
[g] Department of Cardiology, HELIOS Clinic Wuppertal, University Hospital Witten/Herdecke, Wuppertal, Germany
[h] Hannover Medical School, Hannover, Germany

ARTICLE INFO

Keywords:
Autonomic dysfunction
Heart failure
Heart rate variability
Baroreflex sensitivity
Animal model
Digital technologies

ABSTRACT

Despite medical advances in the treatment of heart failure (HF), mortality remains high. It has been shown that alterations of the autonomic-nervous-system (ANS) are associated with HF progression and increased mortality. Preclinical models are required to evaluate the effectiveness of novel treatments modulating the autonomic imbalance. However, there are neither standard models nor diagnostic methods established to measure sympathetic and parasympathetic outflow continuously. Digital technologies might be a reliable tool for continuous assessment of autonomic function within experimental HF models.

Telemetry devices and pacemakers were implanted in beagle dogs ($n = 6$). HF was induced by ventricular pacing. Cardiac hemodynamics, plasma catecholamines and parameter describing the ANS ((heart rate variability (HRV), deceleration capacity (DC), and baroreflex sensitivity (BRS)) were continuously measured at baseline, during HF conditions and during recovery phase.

The pacing regime led to the expected depression in cardiac hemodynamics. Telemetric assessment of the ANS function showed a significant decrease in Total power, DC, and Heart rate recovery, whereas BRS was not significantly affected. In contrast, plasma catecholamines, revealing sympathetic activity, showed only a significant increase in the recovery phase.

A precise diagnostic of the ANS in the context of HF is becoming increasingly important in experimental models. Up to now, these models have shown many limitations. Here we present the continuous assessment of the autonomic function in the progression of HF. We could demonstrate the advantage of highly resolved ANS measurement by HR and BP derived parameters due to early detection of an autonomic imbalance in the progression of HF.

Abbreviations: ANS, autonomic nervous system; BP, blood pressure; BPM, beats per minute; BRS, baroreflex sensitivity; DC, decleration capacity; DPB, diastolic blood pressure; ECG, electrocardiogram; GSD, geometric standard deviation; HF, heart failure; HFpEF, heart failure with preserved ejection fraction; HFrEF, heart failure with reduced ejection fraction; HPLC, high-performance liquid chromatography; HR, heart rate; HRR, heart rate recovery; HRV, heart rate variability; LF, low-frequency; LVEDP, left ventricular end-diastolic pressure; LVEDV, left ventricular end-diastolic volume; LVEF, left ventricular ejection fraction; LVESV, left ventricular end-systolic volume; LVP, left ventricular pressure; LVSP, left ventricular systolic pressure; MAPSE, mitral annular systolic excursion; MBP, mean blood pressure; NA, norepinephrine; PET, positron emission tomography; pNN50, percentage of long RR-intervals diverging from each other by >50 ms; PNS, parasympathetic nervous system; RMSSD, root-mean-square of the SDNN; SBP, systolic blood pressure; SDNN, standard deviation of the RR-intervals; SNS, sympathetic nervous system; SPECT, single photon emission computed tomography; TAU, time constant for isovolumetric relaxation.

* Corresponding author at: Bayer AG, Research & Development, Pharmaceuticals, Cardiovascular Precision Medicine 2, BAG-PH-RD-RED-TA1-CPM-CPM2, Aprather Weg 18a, D-42096 Wuppertal, Germany.
E-mail address: thomas.mondritzki@bayer.com (T. Mondritzki).

https://doi.org/10.1016/j.vascn.2023.107480
Received 6 August 2023; Received in revised form 8 November 2023; Accepted 13 November 2023
Available online 16 November 2023

1. Introduction

Due to effective treatments of ischemic heart diseases and an advancing life span nowadays, morbidity and mortality for chronic heart failure (HF) are continuously rising (Benjamin et al., 2018; Ziaeian & Fonarow, 2016). HF is a complex clinical syndrome and is defined as the inability of the heart to provide the organism with an adequate blood flow (Benjamin et al., 2018). With a prevalence of 38 million patients worldwide, HF remains the leading cause of hospitalization and rising health expenditure (Ziaeian & Fonarow, 2016).

In HF patients, the sympathetic nervous system (SNS) is enormously upregulated, whereas the parasympathetic nervous system (PNS) is downregulated (Eckberg, Drabinsky, & Braunwald, 1971). This initial adjustment of the autonomic nervous system (ANS) is an adaptive mechanism to maintain a sufficient cardiac performance (van Bilsen et al., 2017). However, a persistent ANS imbalance leads to maladaptation, deteriorates HF progression, and might finally lead to higher mortality rates in the affected patients (Florea & Cohn, 2014; Triposkiadis et al., 2009).

Several therapy options have been developed to counteract the

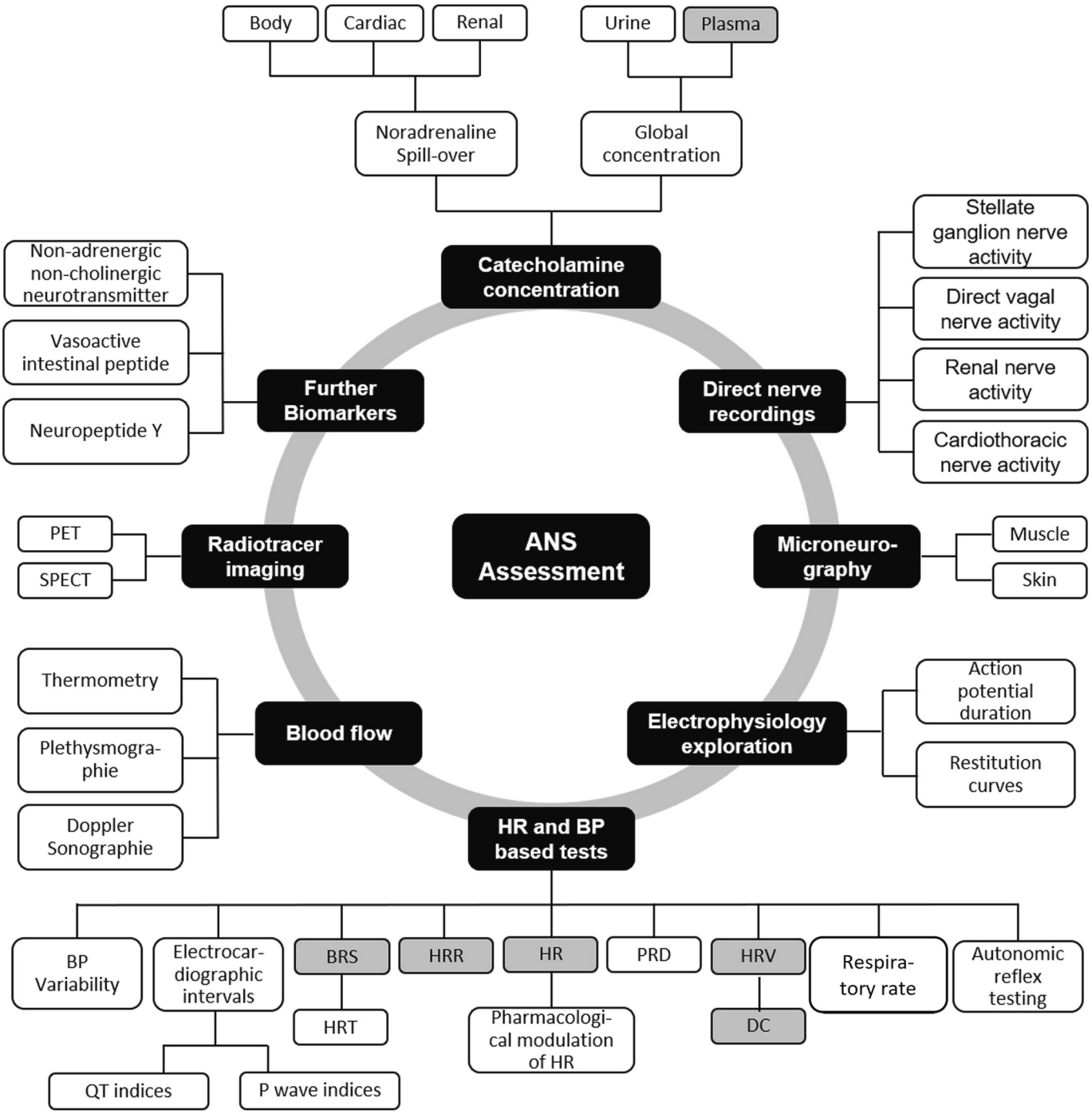

Fig. 1. Methods of ANS assessment. HR = heart rate, BP = Blood pressure, BRS = baroreceptor sensitivity, HRT = heart rate turbulence, HRR = heart rate recovery, PRD = periodic repolarization dynamics, HRV = heart rate variability, DC = deceleration capacity, PET = positron emission tomography, SPECT = single photon emission computed tomography. Autonomic reflex testing sums up clinical tests such as Valsalva maneuver, isometric hand-grip test, head-up tilt test, etc. As these tests are not suitable for preclinical use, they are not shown in this figure. Methods we address in this study displayed in grey.

imbalance of the ANS: Pharmacological approaches are based on modulations of the sympathetic outflow by β-blockers which are an established component of heart failure therapy (McDonagh et al., 2021). Enhancement of the parasympathetic branch by i.e., acetylcholine esterase inhibitors has been explored in experimental models (Khuanjing, Palee, Chattipakorn, & Chattipakorn, 2020; van Bilsen et al., 2017). In recent years, new approaches, such as vagus nerve stimulation, renal sympathetic denervation, spinal cord stimulation, stellate ganglionectomy, and baroreceptor stimulation have been the subject of many studies (Byku & Mann, 2016; Schwartz, La Rovere, De Ferrari, & Mann, 2015; Tsioufis et al., 2017). These device-based techniques reveal to be promising new therapies, and their use seems to be safe in humans (Wagner & Frishman, 2018). However, despite promising results from preclinical animal studies, some study results could not be transferred to the clinical situation (Hanna, Shivkumar, & Ardell, 2018; Tsioufis et al., 2017).

To improve the transferability from early research studies into the clinical setting, predictive animal studies are of considerable relevance regarding the determination of efficacy and estimation of effect sizes as well as identification of effect-onset and duration. To adequately investigate potential therapeutic approaches, a detailed understanding of the ANS under healthy as well as pathophysiological conditions should exist.

For this purpose, a variety of methods assessing the different branches of the ANS are available. Fig. 1 provides an overview of methods to assess cardiac autonomic function. Several of these techniques e.g., cardiac sympathetic radiotracer imaging and sympathetic nerve recordings are less commonly used in clinical practice (Goldberger, Arora, Buckley, & Shivkumar, 2019; Patel et al., 2013; van Bilsen et al., 2017). In addition, not all diagnostic approaches are reversely translatable from the clinical setting to preclinical research. E.g., microneurography can only be performed in anesthetized animals. However, anesthesia causes artifacts in cardiac hemodynamics (Vatner & Braunwald, 1975). Additionally, these data can only be recorded over a very short period. Recording direct nerve activity allows direct evaluation of sympathetic or vagal nerve activity (Au - Hamza SM, Au - Hall JE., 2018; Boehler, Carli, Fadiga, Stieglitz, & Asplund, 2020; Stieglitz, 2020). However, this method requires implantation of additional electrodes and thus another surgery (Au - Hamza SM, Au - Hall JE., 2018). In addition, there has been limited standardization regarding electrodes, and translation from preclinical studies to clinical trials in this area is often still difficult (Boehler et al., 2020; Stieglitz, 2020). Nevertheless, this method is expected to become increasingly used in research in the next few years. Overall, preclinical studies often deliver limited insights into the pathophysiology of ANS imbalance in HF and potential treatment options. Due to these methodological restrictions, the transferability of results from preclinical studies into the clinic can be limited (Hart et al., 2017). Apart from invasive methods such as microneurography, non-invasive techniques for heart rate- (HR-) based measurements of autonomic function are increasingly being explored.

In animal studies, there is less consistent evidence to what extent ANS parameters change in terms of HF characteristics, compared to established markers like LVEF. In preclinical studies, in addition to biomarkers such as plasma norepinephrine level (NA), indices derived from hemodynamic parameters such as heart rate variability (HRV) and baroreflex sensitivity (BRS), and to some extent direct nerve activity have been investigated (Dunlap, Kinugawa, Sica, & Thames, 2019; Ishise et al., 1998; Motte et al., 2005; Ootaki et al., 2008; Piccirillo et al., 2018; Zhang et al., 2009). The tachypacing model is a standard model, which serves as a model for dilated cardiomyopathy (Charles, Rademaker, Scott, & Richards, 2020; Dixon & Spinale, 2009; Recchia & Lionetti, 2007; Spannbauer et al., 2019). For drug-induced BRS, this model showed a reduction during tachypacing-induced heart failure (Dunlap et al., 2019; Zhang et al., 2009). For parameters of HRV, on the other hand, the results are partially heterogeneous. For low-frequency band from the frequency domain of HRV, partially decreased values (Motte et al., 2005; Ootaki et al., 2008) and partially increased values (Binkley, Nunziata, Haas, Nelson, & Cody, 1991; Ishise et al., 1998; Piccirillo et al., 2018; Zhang et al., 2009) are described during tachypacing. In contrast, the high-frequency band consistently appears to be decreased (Binkley et al., 1991; Ishise et al., 1998; Motte et al., 2005; Ootaki et al., 2008; Zhang et al., 2009). For the biomarkers NA, sometimes no increase during heart failure and sometimes a delayed increase are described in the progression of HF induced by tachypaching (Dunlap et al., 2019; Zhang et al., 2009; Zucker et al., 2007). Individual studies show a direct increase in NA after pacing onset (Lopshire & Zipes, 2014). Overall, most studies investigate single of the mentioned parameters and mostly relatively few measurement time points were chosen during pacing. Pacing regimes also vary to some extent, for example, pacing was performed at different frequencies and pacing periods also range from 2 weeks to 8 weeks. To our knowledge, newer parameters for monitoring autonomic dysfunction such as deceleration capacity (DC), as well as exercise-dependent tests such as heart rate recovery (HRR) have not been investigated at all in preclinical studies. As previously described, the high heterogeneity of applied methods and the lack of validated protocols impairs a successful translation of preclinical results into clinical practice.

Out of the diversity of measurement methods, it is essential to identify reliable methods to assess parameters of ANS activity and to estimate the effect size for a given pathophysiological condition to evaluate new therapy approaches. Therefore, telemetry devices acquire greater popularity in preclinical research to measure cardiac hemodynamics and ANS activity continuously in conscious animals. Here we hypothesized, that a) the implementation of telemetry sensors into preclinical disease models delivers cardiac hemodynamic data as well as contemporaneous data describing the ANS (HRV, BRS, DC, HRR) without the influence of anesthesia b) thereby this approach could further allow a direct and temporally high-resolution correlation of heart function versus ANS outflow and c) estimate the effect size of an autonomous dysregulation for a given cardiac disease and vice versa.

In the present study, we investigate the time course of established ANS parameters such as HRV, BRS, biomarker NA, as well as exercise-dependent HRR and novel parameters such as DC, parallel to hemodynamic changes in a tachypacing-induced HF model.

2. Material and methods

2.1. Ethics statement

All study procedures complied with the current national legislation (German protection of animals' act [May 18, 2016], last amended by article 4 paragraph 87 [BGB1. I S. 1666] on July 18, 2016, and the EU directives 63/2010 [on the protection of animals used for scientific purposes]). All performed study protocols were approved by the competent regional regulatory authority (LANUV NRW in Duesseldorf/Germany) and by the institutional animal care office of the Bayer AG. The investigation conforms to the Guide for the Care and Use of Laboratory Animals published by the US National Institutes of Health (publication no. 85–23, revised 1985).

None of the animals were euthanized during this study and all animals recovered from HF conditions.

2.2. Animal model and data collection

To examine suitable parameters describing the ANS activity, we have chosen a tachypacing-induced HFrEF (heart failure with reduced ejection fraction) model in male dogs. This model has been well characterized for decades and shows typical features of dilated cardiomyopathy (Mondritzki et al., 2018) Advantages of this model are the controllability of disease manifestation and the low variability in HF relevant outcome parameters. For long-term monitoring of HRV and BRS parameters we included telemonitoring systems in the study concept, to receive all data

from conscious animals. Furthermore, blood samples were collected to determine appropriate biomarkers (adrenaline, noradrenaline) and to compare these `conventional´ readouts with hemodynamically derived data.

2.3. Overall study protocol

As shown in Fig. 2, pacemaker and telemetry sensors were implanted in dogs ($n = 6$ animals) as described below. After wound healing, all animals were studied in the awake state during healthy conditions, HF conditions, and a recovery period. HF was induced by tachypacing over 42 days: 28 days with 220 bpm followed by 14 days with 180 bpm. Finally, all dogs were investigated for further 49 days during recovery.

To evaluate the hemodynamic consequences of HF on cardiac performance, blood pressure (BP) and heart rate (HR), hemodynamics were telemetrically recorded twice a week before and during the whole pacing-period. In the first week of recovery, telemetry recordings were performed throughout the time. Measurements were conducted for 23 h (h) (10:00–9:00 the following day) during normal housing conditions. During the pacing-interval, pacemakers were turned off for 1 h to allow measurements under spontaneous rhythms. Blood samples were taken weekly during the pacing phase and at two time points during the recovery phase. Echocardiography was implemented on day −14, 14, 28, 42. Exercise studies were performed at two time points during baseline (day −14, −7) and at three time points during the pacing interval (day 14, 28, 42). All data were recorded and analyzed using the software Ponemah ® (Version 5.2, Data Sciences International, USA).

2.4. Pacemaker and telemetry sensor implantation

Six healthy male *beagle* dogs (Marshall BioResources, USA), weighing between 10 and 15 kg, were equipped with pacemakers (Logos, Biotronik, Germany) and telemetry sensors (L21, Data Science International, USA). Therefore, animals were intubated and mechanically ventilated by an Avance anesthesia ventilator (GE Healthcare, Germany) applying 30% oxygen and anesthetic gas during all surgical procedures. Anesthesia was initiated by Thiopental-Na (0.25–0.5 mg/kg, Trapanal, BYK Gulden, Germany) and maintained by isoflurane (1.0–2.0%; Isoflurane Baxter, Baxter Germany). For analgesia, fentanyl (10–40 μg/kg per hour, Mallinckrodt Inc) was infused intravenously.

A pacemaker lead (Setrox S60, Biotronik, Germany) was inserted under x-ray guidance (OEC FlexiView 8800, GE Healthcare) through the right jugular vein and anchored in the right ventricle. The pacemaker was sutured subcutaneously between the shoulder blades and connected with the electrodes. Subsequently, intracardiac signals were measured to ensure successful implantation.

For telemetry implantation, a left-sided thoracotomy was conducted. Afterwards, one pressure sensor was placed in the thoracic aorta to measure central BP. By insertion of a second pressure catheter in the left ventricle, left ventricular pressure (LVP) can be recorded. Finally, two electrocardiography (ECG) leads were sutured onto the pericardium.

All surgical procedures were performed under aseptic conditions, and all animals received an antibiotic (150 mg/d, Clindamycin hydrochloride (Clerobe®, (Zoetis, Parsippany, USA)) and analgesic (50 mg/d Carprofen p.o. (Rimadyl®, Pfizer, USA)) medication post-operative over a period of 10 days. Additional analgesia was ensured by a Durogesic® patch (25 μg/h Fentanyl, Janssen-Cilag GmbH, Neuss, Germany) on the right thoracic wall.

2.5. HF assessment: hemodynamic, echocardiography, biomarkers

The hemodynamic changes during HF progression were monitored by the recording of systolic (SBP), diastolic (DBP) and mean (MBP) blood pressure as well as LVP and ECG signals. Further parameters, e.g., HR, left ventricular contractility and relaxation and cardiac output (CO) were derived from these data. Each parameter was averaged for the 1 h-pacing-free interval. To characterize the extent of HF in more detail, LVEF was determined by transthoracic 2-dimensional echocardiography (Ultrasound device: GE Healthcare, Model S5; Ultrasound probe: GE Healthcare, Model 12S) fortnightly. From 2- and 4-chamber views, the LVEF was determined according to the Simpson method using the software EchoPAC™ (GE Healthcare) Left-ventricular dysfunction has also been characterized by weekly measurements of Nt-pro-BNP from venous blood samples using Cardiopet pro BNP Elisa kits (IDEXX Laboratories, Germany).

2.6. ANS assessment

HR, HRR, HRV, DC and BRS were calculated from the continuously recorded ECG and BP signals in the pacing-free interval, if not specified otherwise.

2.7. Heart rate

The most feasible way to assess autonomic function is HR measurement. The HR is a response to autonomic control in terms of different conditions, like circadian rhythm, exercise and temperature, and might also be influenced by pathophysiological conditions. An elevated HR is driven by the sympathetic branch and conversely, a HR reduction is mediated by the parasympathetic branch (Patel et al., 2013).

In this study, HR was calculated from ECG recordings using the Ponemah® software (Data Science International, Version 5.2, USA). In the pacing free interval, HR was recorded at spontaneous rhythm in all animals.

2.8. Heart rate variability

HRV is a further important diagnostic readout of ANS balance, describing the variations in the interval between individual heart beats caused by alterations in the ANS (*Circulation.*, 1996; van Bilsen et al., 2017). HRV can be assessed by analysis of time as well as frequency domain parameters. Time-domain parameters such as the standard

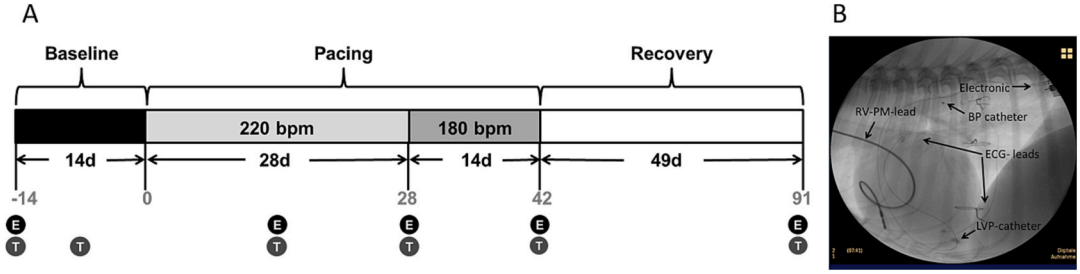

Fig. 2. Study protocol and sensor implantation. (A) A schematic overview of the time course of the study. E = echocardiography, T = treadmill exercise (B) X-ray of the thorax with implanted telemetry device and pacemaker. The blood pressure catheter (BP catheter) was inserted in the aorta, the left ventricular pressure catheter (LVP-catheter) in the left ventricle. ECG leads were sutured onto the pericardium. The pacemaker electrode (RV-PM-lead) was placed in the right ventricle.

deviation of the RR-intervals (SDNN), the root-mean-square of the SDNN (RMSSD) and the percentage of long RR-intervals diverging from each other by >50 ms (pNN50) can be derived from RR-intervals (*Circulation.*, 1996). SDNN reflects the whole ANS activity and is an indicator of overall HRV. RMSSD and pNN50, indicate short-term and spontaneous variability and are assigned to parasympathetic activity (Pumprla, Howorka, Groves, Chester, & Nolan, 2002). The frequency-domain analysis subdivides HRV into a high-frequency band (HF) reflecting parasympathetic activity, a low-frequency band (LF) representing parasympathetic but predominantly sympathetic activity and a very-low-frequency band, that appears to reflect parasympathetic activity, in addition to thermoregulatory and renin-angiotensin influences. (Akselrod et al., 1981; Shaffer & Ginsberg, 2017).

However, recent studies have shown that the assignment of these parameters to parasympathetic, sympathetic and overall activity seems to be oversimplified (Hayano & Yuda, 2019). Furthermore, the various measurement methods, such as long- and short-term according impair the comparability of the results (Notarius & Floras, 2001; van Bilsen et al., 2017). Despite these limitations, it is presumed that HR variations are ANS modulated, and thus HRV parameters provide insights into the autonomic (im-) balance (Hayano & Yuda, 2019).

Here, time domain and frequency domain analysis were performed with the Notocord-hem™ software (version 4.3.0.75). For time-domain analysis SDNN, RMSSD and pNN50 were determined as averages of the pacing free hour (h). Parameters of frequency domain were calculated by power spectral analysis. Five-minute sections were required to perform Fast-Fourier-transformation to determine high-frequency band (HF-band) and low frequency band (LF-band). These sections were also obtained from the pacing-free interval and plotted as averages. The high-frequency band as a parameter of parasympathetic nerve activity was defined from 0.15 to 0.5 Hz; the low-frequency band was associated to SNS and PNS activity with a prior weighting on SNS activity, was defined from 0.04 to 0.15 Hz. The very-low-frequency band ranges from 0 to 0.04 Hz. Total power (TP) was defined from 0 to 0.5 Hz.

2.9. Deceleration capacity

DC is a HRV- parameter which was discovered more recently. DC seems to reflect tonic PNS influences on the sinus node (Bas et al., 2015; Bauer et al., 2006a). Thus, analysis of deceleration-related HRV might allow for a distinction between parasympathetic and sympathetic influences on the ANS (Bauer et al., 2006a). Reduced DC derived from short-term as well as 24 h measurements is a strong independent predictor for mortality after MI (Rizas et al., 2018). In patients with dilatative cardiomyopathy, DC has shown to be a predictive factor for HF exacerbation (Zou et al., 2016). To our knowledge, DC has not previously been investigated in a canine HF model. In the present study we show the amplitude and the progression of DC during the pacing-induced development of HF and the recovery phase.

DC was calculated by using the phase-rectified signal averaging (PRSA) – a technique described by Bauer and colleagues (Bauer et al., 2006b). By defining anchor points, windows around each anchor point as well as aligning and averaging these windows, PRSA curves were obtained. These were further processed in MATLAB (Version R2018b, USA) to provide the deceleration capacity. Large values >5000 ms were excluded to devoid measurement artifacts.

2.10. Heart rate recovery

Another parameter derived from hemodynamic measurements is HRR. HRR is defined as the decline in HR after maximal exercise and reflects the ability of parasympathetic reactivation (Imai et al., 1994; Pierpont & Voth, 2004). An attenuated HRR could be found in HF patients frequently and is considered to have a prognostic impact for all-cause mortality (Cole, Blackstone, Pashkow, Snader, & Lauer, 1999).

To study this important parameter all dogs were trained to perform a treadmill exercise starting with a 3-min baseline, followed by a 2-min run at a slope of 6° and a maximal velocity of 6.4 km/h. The run was divided into 30 s of steady speed increase and 90 s at full speed. The exercise was followed by a recovery phase of 5 min. The same procedure was then repeated with a slope of 12°. For HRR, HR was calculated from the LVP signal which was continuously recorded by the telemetry device. Exercise was performed at healthy state and during the high-pacing interval (220 bpm/min) on day 14 and 28 and in the low-pacing phase (180 bpm/min) on day 42 after the start of pacing. Each exercise test was performed in the pacing-free interval.

2.11. Spontaneous Baroreceptor sensitivity

BRS is a regulatory mechanism to maintain arterial BP driven by arterial baroreceptors registering any changes in BP. A rise in BP for instance leads to an increased vagal tone and a decreased sympathetic activity. Conversely, a drop in BP promotes contrarious changes in autonomic activity. Thereby, the baroreflex is immediately mediated by the parasympathetic branch whereas the sympathetic branch reacts with a delay. Thus, BRS is mainly exerted by the PNS (La Rovere, Pinna, & Raczak, 2008).

For spontaneous BRS calculation, a baroreflex sequence analyzer from Notocord-hem™ (version 4.3.0.75, module BRS10a) was used. Using the automated sequence method changes and in SBP followed by a lengthening or shortening in the RR-I of at least 3 consecutive beats were identified. Data with a linear correlation coefficient of <0.85 between SBP and RR-I were excluded. The baroreflex sequence analyzer extracts baroreflex slope (ms/mmHg). The BRS is expressed as the average of all slopes.

2.12. Catecholamine plasma level

Elevated plasma noradrenaline (NA) levels are indicative of excessive sympathetic activity during HF. But only a proportion of NA released from the synaptic cleft reaches into the blood plasma. Furthermore, NA plasma concentrations depend not merely on NA release but also on its elimination in the plasma (Esler et al., 1984). Thus, plasma NA levels may not provide a specific assessment of cardiac sympathetic innervations. Therefore, the benefit of NA plasma levels as a biomarker for SNS activity is limited (van Bilsen et al., 2017).

Nevertheless, increased plasma NA levels are associated with an increased mortality in HF patients and seem appropriate for a rough estimation of the cardiac sympathetic innervations (Cohn et al., 1984; Kaye et al., 1995; van Bilsen et al., 2017).

Venous blood samples were collected weekly during pacing with 220 bpm, afterwards over longer intervals to determine plasma noradrenaline (NA) levels. The blood samples were stored at −20 °C after centrifugation at 4000 rpm for 10 min, until further analysis was performed. Plasma was processed for HPLC (high-performance liquid chromatography) based determination of catecholamines at MLM Medical Labs GmbH (Moenchengladbach, Germany).

2.13. Statistical analysis

Statistical data analysis and graphical representation were done using the GraphPad Prism software (Version 8, GraphPad Software Inc). All data were expressed as mean +/− SD in tables or geometric mean +/− geometric standard deviation (GSD) in figures. Normal distribution was tested using logarithmic transformation. Differences between healthy and disease state were determined with repeated measures using the one-way ANOVA test. In case of missing values due to technical issues, mixed-effects analysis was performed to compare baseline data with data during pacing phase and recovery phase on every occasion of measurement. For significant differences ($P < 0.05$) between baseline, HF phase, and recovery phase, Dunnett's multiple comparison test was used at each time of measurement. The Dunnetts test was performed

when the ANOVA test demonstrated significant levels. Furthermore, averages were calculated for the respective pacing regimes to provide a general trend for HF conditions. Repeated-measures one-way ANOVA was performed to compare the baseline data with the averaged data during the pacing phase and recovery phase. Dunnett's multiple comparison test was used for significant differences ($P < 0.05$) between baseline, HF phase and recovery phase.

3. Results

Using high-resolution telemetry technology, continuous hemodynamic monitoring of all animals was possible during the complete time course of the study. At single time points, data dropouts occurred in some animals due to excessive movement of the animals and consequent poor signal quality. The blood pressure sensor was not functional after implantation in one animal and showed no signal. Overall, data from at least 5 animals could be included in the analysis. Due to technical reasons hemodynamic data points of individual animals could not be recorded on day 4, 8, 11, 15, 45 and 47. On these days, the group size was $n = 5$. All data demonstrates lognormal distribution, and subsequently an ANOVA test for normally distributed data could be performed.

3.1. Model characteristics

Table 1 summarizes cardiac hemodynamics, echocardiography data and Nt-proBNP plasma levels of selected time points during baseline, pacing and recovery phase. All animals showed the expected changes in HF relevant parameters.

The HR significantly increased by 21.1 ± 4.8% averaged over the entire pacing phase. The recovery phase showed a decrease in HR compared to baseline of −11 ± 2%. Compared to baseline contractility was significantly decreased by −54 ± 4% during the pacing phase. Significant deviations were identified at the first day of pacing. A reduction of −50 ± 8% was achieved already 4 days after the start of pacing. During recovery, the contractility approached to baseline again. Relaxation and time constant for isovolumetric relaxation (TAU) followed similar tendencies as they showed significant changes of −48 ± 5% (-dP/dt) and + 45 ± 16% (TAU) during pacing and renewed to baseline levels during the recovery phase. SBP and LVSP showed a significant average decrease during pacing by −33 ± 6% and − 18 ± 5% respectively ($P = 0.0102$ for SBP and $P = 0.0014$ for LVSP). Compared to baseline, a significant reduction in LVEF of −47 ± 2% was observed during pacing. Nt-proBNP levels significantly increased from 423.7 ± 74.75 pmol/l at baseline to a maximum of 5876 ± 1611 pmol/l during pacing. In summary, these results confirm tachypacing-induced HF in all animals.

3.2. Assessment of autonomic function

3.2.1. HRV: SDNN, pNN50, RMSSD, HF, LF, TP, DC

As shown in Figs. 3 and 4, time-domain (Fig. 3) and frequency-domain parameters (Fig. 4) of HRV were determined during baseline, pacing and recovery phase.

Compared to baseline, RR-I and SDNN were significantly reduced during pacing. During the high pacing phase of 220 bpm the RR-I showed an average reduction of −19 ± 2% compared to baseline. During the low pacing with 180 bpm phase RR-I decreased by −14 ± 3% compared to baseline. On average, a noticeable reduction in SDNN of −49 ± 6% was observed during high pacing. During low pacing, an average reduction in SDNN of −36 ± 5% compared to baseline was observed. Compared to the pre-pacing period RMSSD and pNN50 as parameters presumably describing PNS activity were reduced during the pacing phase. The reduction in RMSSD during high pacing ranged from 47 ± 29% to 63 ± 15% compared to baseline. Simultaneously pNN50 showed an average decrease of −47 ± 9% (high pacing) and − 31 ± 9% (low pacing), indicating a showed a significant effect compared to baseline. In general, the determination of RMSSD and pNN50 provided

Table 1
Model characteristics by echocardiography, biomarkers and hemodynamic parameters during baseline, pacing-induced heart failure and recovery measured on predefined time points. All data are expressed as $n = 5–6 \pm$ SD., $^*P < 0.05$ for comparison with mean of baseline.

Parameter/week	Baseline	RV-Pacing 220 bpm				180 bpm	Recovery		
		1	2	3	4	5	7	8	13
Contractility [dP/dt$_{max}$; mmHg/s]	3754 ± 489.5	2495 ± 564.2*	1812 ± 131.1*	1750 ± 196.1*	1723 ± 202.8*	1893 ± 238*	2506 ± 512.8*	3627 ± 891.2	3278 ± 691
HR [bpm]	93.83 ± 8.374	119.6 ± 11.83	110.2 ± 8.25	112 ± 3.085	109.3 ± 4.502	109.2 ± 9.065	89.31 ± 11.41	79.81 ± 4.265*	86.14 ± 13.89
Relaxation [dP/dt$_{min}$; mmHg/s]	−3652 ± 806.6	−2666 ± 399.3*	−2204 ± 232.3*	−1985 ± 353.8*	−1918 ± 247.7*	−2076 ± 316.9*	−2697 ± 377.6*	−3322 ± 409.1	−3298 ± 473
LVEDP [mmHg]	17.51 ± 1.946	15.23 ± 3.819	18.08 ± 3.305	25.18 ± 4.382	26.09 ± 8.684	26.48 ± 8.229	24.93 ± 8.464	19.2 ± 10.19	20.69 ± 5.157
TAU [msec]	26.13 ± 2.82	33.73 ± 4.096	33.82 ± 7.153	41.66 ± 3.189	37.04 ± 8.275	40.31 ± 7.168*	30.88 ± 4.901	27.22 ± 4.707	28.25 ± 4.923
SBP [mmHg]	112.8 ± 10.02	98.23 ± 5.54	90.02 ± 8.12	88.91 ± 14.88	86.14 ± 7.96*	88.94 ± 7.64*	96.61 ± 5.42*	104.2 ± 5.84	112.2 ± 11.06
DBP [mmHg]	78.11 ± 6.53	78.68 ± 8.72	67.76 ± 9.36	67.89 ± 15.59	65.9 ± 8.75	67.08 ± 10.51	68.41 ± 7.18*	68.35 ± 10.52	77.87 ± 12.49
LVSP [mmHg]	126.5 ± 8.51	110.5 ± 7.87*	105.5 ± 7.61*	107.8 ± 11.91*	102.6 ± 7.02*	104.9 ± 8.18*	114.7 ± 4.76*	121.7 ± 9.76	128.3 ± 6.51
Nt-proBNP [pmol/l]	423.7 ± 74.75	3296 ± 602.8	4891 ± 1510*	5876 ± 1611*	5641 ± 1576*				
LVEF [%]	58.32 ± 4.953		32.27 ± 3.19*		29.28 ± 2.374*	30.32 ± 2.184*			51.28 ± 7.6
MAPSE [cm]	0.67 ± 0.03		0.46 ± 0.04*		0.43 ± 0.08*	0.41 ± 0.08*			0.70 ± 0.02
LVESV [ml]	10.42 ± 2.27		21.12 ± 5.64*		25.95 ± 4.02*	25.67 ± 4.67*			16.18 ± 3.82*
LVEDV [ml]	24.93 ± 3.12		30.96 ± 7.14*		36.83 ± 5.4*	36.73 ± 5.57*			33.62 ± 5.76*

HR = heart rate, LVEDP = left ventricular end-diastolic pressure, TAU = time constant for isovolumetric relaxation, SBP = systolic blood pressure, DBP = diastolic blood pressure, LVSP = left ventricular systolic pressure, LVEF = left ventricular ejection fraction, MAPSE = mitral annular systolic excursion, LVESV = left ventricular end-systolic volume, LVEDV = left ventricular end-diastolic volume.
Hemodynamic data are shown for baseline and day 1, 8, 15, 22, 29, 43, 49, 90 during pacing and recovery phase.

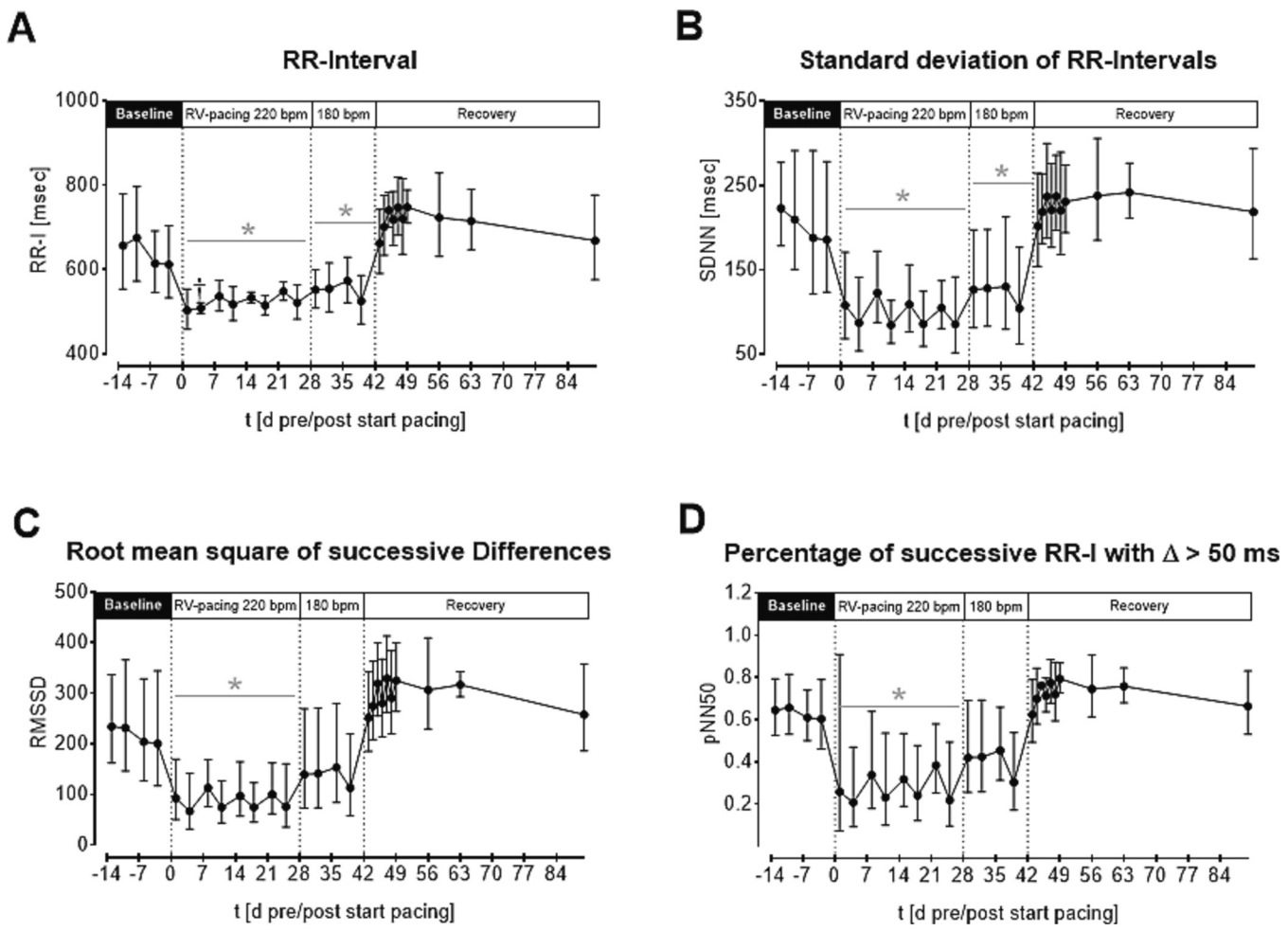

Fig. 3. Time course for changes in time domain parameters of HRV through the entire study. All data points expressed as geometric mean ± GSD for $n = 5$–6 dogs. *$P < 0.05$ for comparison with mean of baseline. (A) RR-intervals, (B) SDNN = standard deviation of the RR-intervals, (C) RMSSD = root-mean-square of the standard deviation, (D) pNN50 = percentage of long RR-intervals, diverging from each other by >50 ms.

data with high variance. In the recovery phase, an overshooting increase of the time domain parameters was observed.

Power spectral analysis was performed to eliminate HR dependency and to differentiate the frequency domain parameters. The time course of frequency domain parameters is summarized in Fig. 4. The low-frequency-band decreased by 69 ± 11%. The detected decrease was significant for most measurement points. The very-low-frequency band is reduced by 37 ± 21% on average from baseline during pacing. In the high-frequency band a decline of −73 ± 10% was revealed during high pacing and, −61 ± 6% during low pacing, respectively. On average, the pacing phase showed a significant effect compared to baseline. Furthermore, total power decreased by −67 ± 12% on average and 58 ± 7% compared to baseline.

Compared to baseline DC was decreased during pacing. A significant reduction of up to −67 ± 16% on day 25 was detected. A reduction of −56 ± 1% compared to baseline could be observed for the entire pacing phase. On average, a reduction in DC from baseline of −56 ± 10% could be observed.

All data points expressed as geometric mean ± GSD for $n = 5$–6 dogs. *$P < 0.05$ for comparison with mean of baseline. (A) VLF = very-low frequency band (B) LF = low frequency band, (C) HF = high frequency band, (D) TP = Total power, (E) LF/HF = Low frequency/High frequency ratio, (F) = LF and HF in normalized units (n.U.),

3.3. Heart rate recovery

All animals successfully completed the exercise protocol. The data was recorded on day −14, −7 (healthy state), 14, 28 and 42 (pacing-induced HF) during the pacing free hour.

At healthy state during the maximal velocity at a 6° slope, the HR averaged 181 ± 12 beats per minute (bpm). HR decreased immediately to 51 ± 10 bpm with the stop of the exercise. As shown in Fig. 5, HR decreased by 28 ± 5 bpm during pacing-induced HF. This decline in HRR in animals with HF is significant on day 28 compared to healthy conditions. Similar results could be shown during treadmill exercise at a 12° slope. A significant difference in HRR compared to baseline could be observed already on day 14.

3.4. Baroreceptor sensitivity

Fig. 6 illustrates BRS during the study progress. Spontaneous BRS increased slightly with improved HF and reached the highest BRS level at 55 ± 9 ms/mmHg during the recovery phase. There were encountered considerable intra- and interindividual variances. Thus, no significant deviations from the baseline could be determined during pacing.

3.5. Noradrenaline and adrenaline plasma level

Plasma NA levels obtained during baseline, pacing and recovery phase are shown in Fig. 7A. At the end of the pacing phase NA levels

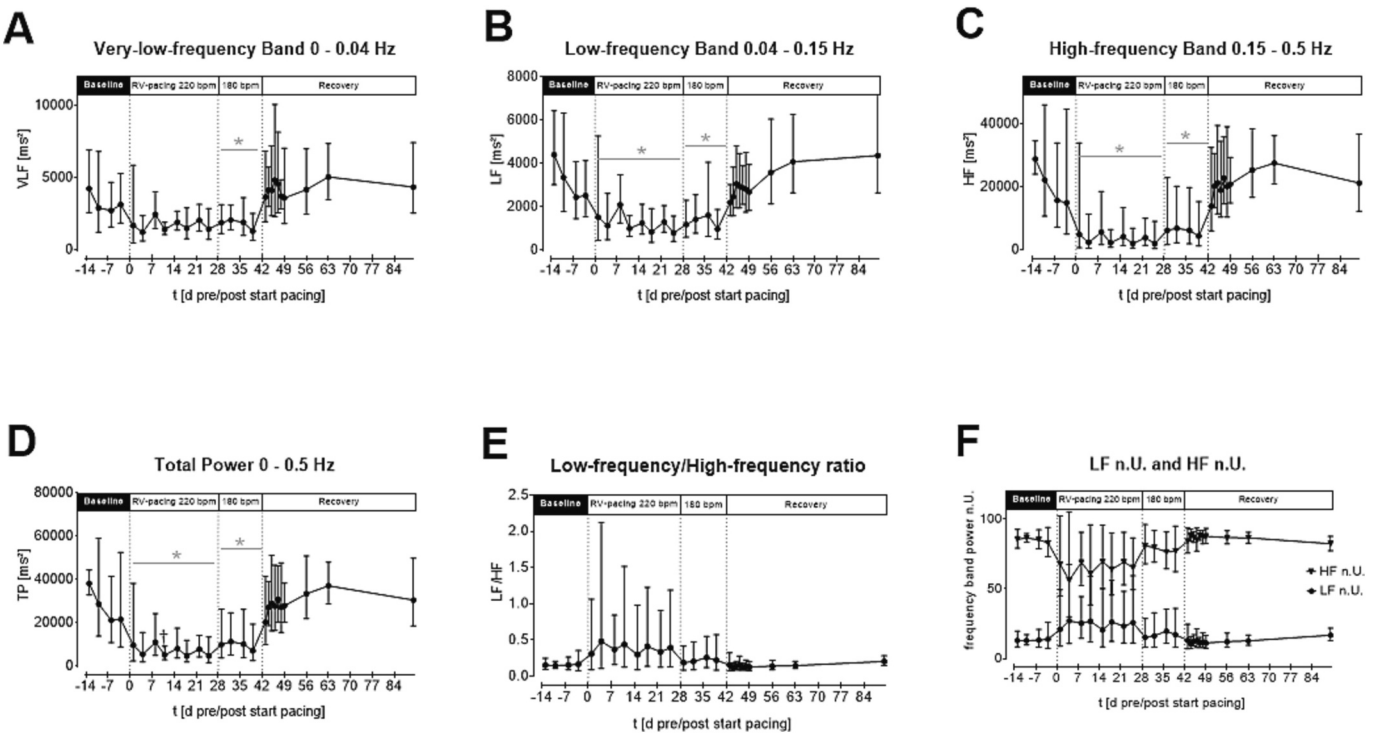

Fig. 4. Time course for changes in frequency domain parameters of HRV through the entire study.

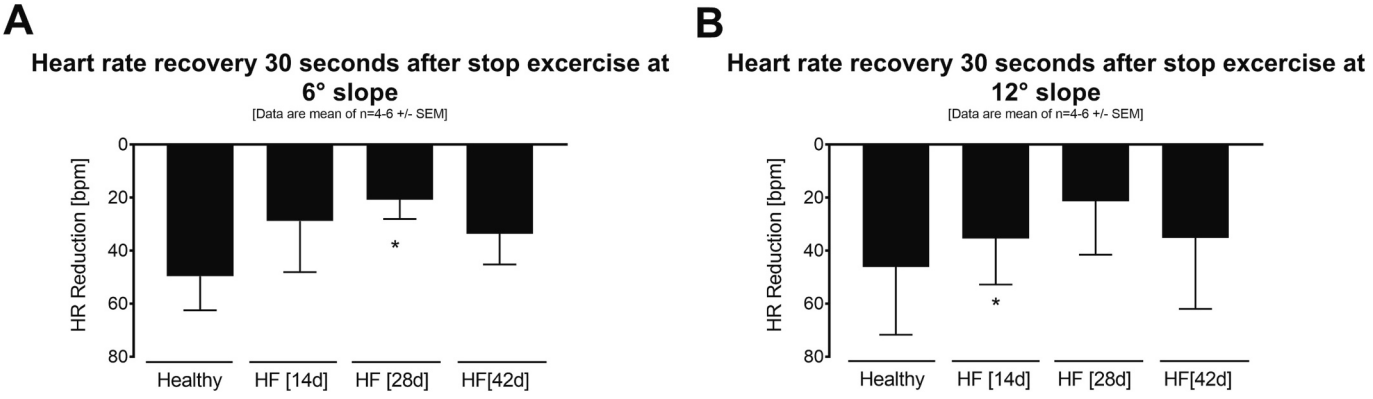

Fig. 5. Heart rate recovery depicted as HR reduction at baseline and at pacing phase and at recovery phase. Values are expressed as geometric mean ± GSD for n = 5–6 dogs. *$P < 0.05$ for comparison with healthy state during baseline.

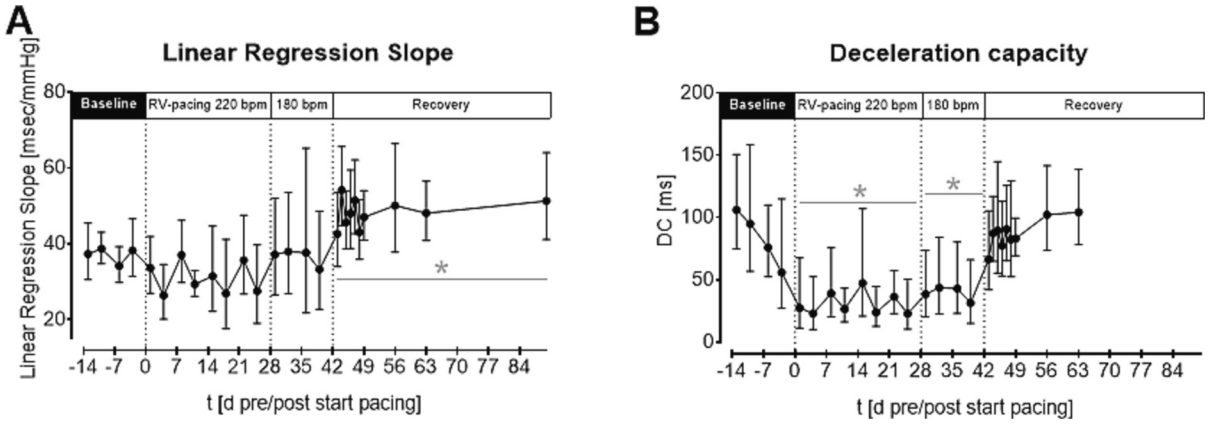

Fig. 6. Time course for changes in baroreflex sensitivity (Fig. 6A) and deceleration capacity = DC (Fig. 6B) during the entire study protocol. All data points expressed as geometric mean ± GSD for n = 5 animals. *$P < 0.05$ for comparison with mean of baseline.

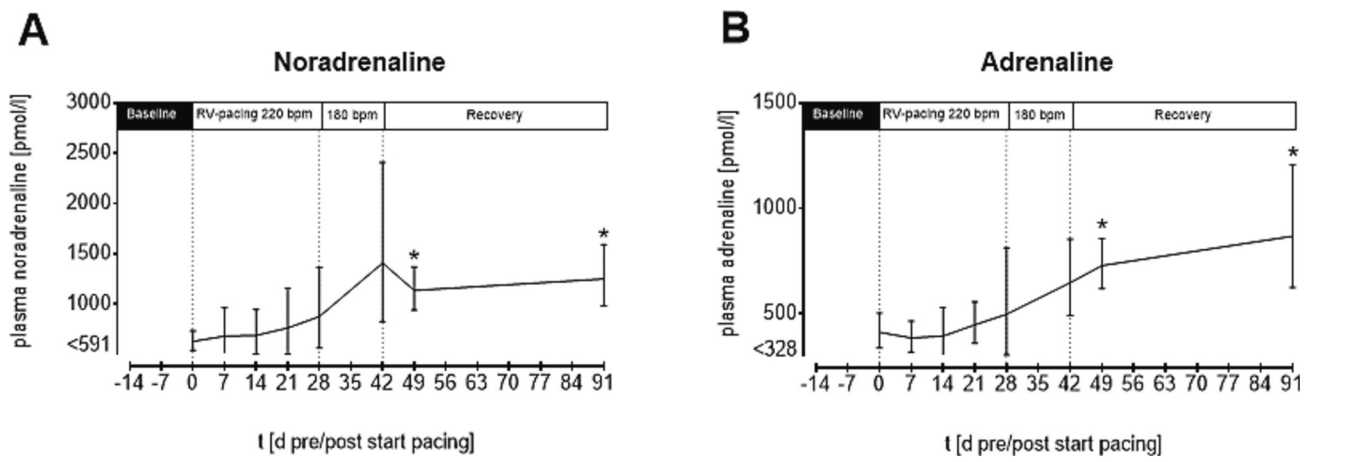

Fig. 7. Noradrenaline and adrenaline levels at baseline, at pacing phase and at recovery phase. Column graph for $n = 6$ dogs. $^*P < 0.05$ for comparison with baseline.

were highly variable but increased to a peak of 1573 ± 694 pmol/l (Reference range 473–2956 pmol/l). After the stop of pacing the NA plasma levels dropped slightly. Plasma adrenaline (Fig. 7B) levels showed a large distribution with slightly rising values in the end of the pacing phase and a further increase up to 906 ± 258 pmol/l in recovery.

4. Discussion

This study aimed to evaluate the time course and effect size of hemodynamically derived parameters and plasma biomarkers of ANS activity. For this purpose, we determined HRV, DC, BRS, HRR and NA-Plasma levels to assess the ANS activity concurrent to classical hemodynamic parameters during the time course of pacing-induced HF in dogs. Major findings were a significant reduction in HRR and DC, reflecting a decrease of the vagal tone, simultaneous to a decline of essential hemodynamic parameters. NA plasma levels showed a delayed response to the increased sympathetic activity. During the recovery phase, the expected increase was observed in all examined HR-derived parameters of ANS activity compared to baseline, synchronous to the parameters characterizing the cardiac function.

The study is limited by the lack of a control group. Instead, we referenced the same animals in healthy status before the animals were affected from disease stimulus. Thus, in terms of the 3R concept, a reduction in the number of laboratory animals could be achieved. Due to the relatively short study duration, no changes in the measured parameters were expected due to e.g. aging of the animals. Nevertheless, confounders and distortions may occur due to the lack of a control group.

The high-resolution telemetrically recorded data allowed us to follow the expected changes in hemodynamic parameters, such as a reduction in contractility, an increase in HR, and a decrease in SBP during the pacing phase. These results are consistent with previous work, describing the same well-approved tachypacing-induced HF model (Coleman et al., 1971; Moe & Armstrong, 1999; Whipple, 1962; Zhang et al., 2009; Zucker et al., 2007). As this HF model is based on tachycardia and results in a HF phenotype of dilated cardiomyopathy, extrapolation of our preclinical results to patients with dilated cardiomyopathy is feasible (Zhang et al., 2009). For other types of HF, i.e. HF after myocardial infarction, further investigations are required.

The deflection of various parameters describing ANS activity has been reported previously in similar animal models (Ishise et al., 1998; Ootaki et al., 2008; Zhang et al., 2009). However, the number of parameters often examined and time points used for measurement were limited (Zhang et al., 2009; Zucker et al., 2007). In several preclinical studies, anesthetic artifacts reduced the transferability of the results into clinical research (Bouairi et al., 2004; Halliwill & Billman, 1992). We present a variety of pathophysiological relevant parameters acquired along the entire time course of the study to closely monitor ANS activity during HF progression.

The expected increase in HR at the start of pacing is a first sign of autonomic dysfunction during the development of HF. But the exclusive determination of HR has limited prognostic value and therefore seems less suitable to evaluate ANS function precisely (van Bilsen et al., 2017). Nevertheless, the elevated HR during the pacing phase is a first indication of autonomic imbalance in the HF model.

For all parameters of HRV, predominantly significant changes were observed with the beginning of pacing. Despite their limitations regarding the correlation of these parameters to a physiological correlate such as sympathetic activity or parasympathetic activity, the changes indicate ANS imbalance during the time course of pacing-induced HF (Coumel & Leenhardt, 1991; Hayano & Yuda, 2019; Ishise et al., 1998; Pagani et al., 1986).

SDNN and TP, commonly assigned to the entire ANS activity, show an early decline in the development of HF, suggesting that ANS imbalance occurs early in the time course of worsening HF. This relationship has already been described in patients (Adamson, 2009; Amorim, 1981).

Frequency domain parameters show significant changes after three days and support a presumed ANS imbalance independent of the HR. During the recovery phase, the restorage of frequency-domain parameters to baseline levels after the stop of pacing, suggests normalization of the HRV. Time-domain parameters indicate enhanced HRV during the recovery phase. But since the HR is diminished after termination of pacing, this conclusion is not entirely valid due to HR dependency of these parameters.

The DC presumably reflecting the parasympathetic activity, declines like the other parameters of HRV with beginning of pacing. In patients, comparable tendencies in HRV have been shown during HF progression (Zou et al., 2016). To our knowledge, no other studies have investigated changes in DC as parameter of parasympathetic nerve activity in a pacing-induced HF model. In accordance with the reduced DC, we find a significant decrease in HRR after 14 days of pacing. As HRR reflects the PNS reactivation after exercise (Pierpont & Voth, 2004), the change in DC seems to be confirmed. Finally, the results from DC and HRR show that parasympathetic activity decreases with the onset of pacing.

Ishise et al. have shown similar effects of parasympathetic withdrawal in a comparable model by the evaluation of HRV (Ishise et al., 1998). Due to the limited informative value of HRV known today (Hayano & Yuda, 2019), conclusions on parasympathetic withdrawal by solely examination of HRV are not appropriate. Regardless of these limitations, our findings are concordant with the results reported previously.

The PNS withdrawal seems to be related to the baroreflex activation

at the beginning of pacing. Since the cardiac output decreases at the beginning of pacing, also the BP decreases significantly. Therefore, the baroreceptors are activated less intensely, resulting in a blunted PNS activation and diminished inhibition of sympathetic nuclei in the medulla oblongata. Consequently, the parasympathetic tonus decreases immediately along with the collapse of cardiac hemodynamics (Ishise et al., 1998). We presume that this mechanism could explain the immediate decrease in the parameters assigned with PNS activity.

Contrarily to HRV parameters, spontaneous BRS was not significantly diminished during the pacing period. Some studies have demonstrated significant decrease in BRS for pacing-induced HF models (Zhang et al., 2009; Zhou, Lei, Fang, Zhang, & Wang, 2009).

Our findings differ from these previously reported data perhaps due to different measurement methods since we used spontaneous BRS in contrast to phenylephrine stimulated BRS used in other studies (Dunlap et al., 2019; Zhang et al., 2009). Iellamo et al. studied spontaneous BRS in conscious dogs with pacing-induced HF and found a significant reduction during HF conditions (Iellamo et al., 2007).However, they did not observe telemetry-equipped animals under normal housing conditions, which may explain the differences in spontaneous BRS.

In addition, it must be considered that all HRV parameters derived from the HR merely describe the influence of the ANS on the sinus node and not the effect on the complete myocardium. Furthermore, these parameters seem to predominantly evaluate the parasympathetic and the entire ANS activity. Therefore, further studies should also consider parameters such as periodic repolarization dynamics that describe the influence of the sympathetic nervous system on the ventricle (Rizas et al., 2019).

Considering biomarkers related to the ANS activity, NA plasma levels showed a delayed increase. Prior studies based on a pacing-induced HF model in dogs have detected changes in ANS activity confirmatory to our results (Ishise et al., 1998; Zucker et al., 2007). Zucker et al. have also shown an increase of NA plasma levels with a delay of about 28 days after the start of pacing, comparable to the findings of this study (Zucker et al., 2007). As NA plasma levels represent the sympathetic activity of the whole organism, it can only be used as a crude indicator for ANS imbalance at later stages of HF progression (Esler et al., 1988).

5. Conclusion

Finally, frequent repetitive measurements of several parameters assessing the ANS function showed that the tendencies described by several authors before can be reproduced in a long-term assessment (Ishise et al., 1998; Ootaki et al., 2008; Zhang et al., 2009; Zucker et al., 2007). Furthermore, based on HRR and the novel HRV-derived parameter DC, we show strong evidence for the diminished parasympathetic activity in this well-described HF model.

We could demonstrate the advantage of continuous high-resolution assessment of the autonomic function in relation to cardiac hemodynamics, using digital technologies to early detect autonomic imbalance in the progression of HF.

Although the mechanisms and pathomechanisms underlying some of the studied parameters have not been sufficiently understood, our data provide valuable insight into the changes of ANS function in experimental HF by simultaneous assessment of various parameters. Many of these parameters have been described in patients showing similar progressions compared to the canine HF model. By analyzing different parameters, the activity of various reflex arcs, involved in ANS imbalance could be estimated in the progression of HF.

This study investigates the effect size of several parameters of ANS function systematically over the entire pacing period and the recovery phase. We presume that the knowledge of the therapeutic window in preclinical studies improves the transferability to clinical studies.

Disclosure instructions

During the preparation of this work the author(s) used no artificial intelligence (AI) or AI-assisted technologies.

Submission declaration and verification

This article has not been published previously, it is not under consideration for publication elsewhere, the publication is approved by all authors and that the article, if accepted, will not be published elsewhere in the same form, in English or in any other language.

Declaration of Competing Interest

The authors declare the following financial interests/personal relationships which may be considered as potential competing interests:

At the time of the study, the following authors were employees of Bayer AG: KB, PP, NW, JB, HTi, JH, HTr, WD and TM.

Data availability

Data will be made available on request.

References

Adamson, P. B. (2009). Pathophysiology of the transition from chronic compensated and acute decompensated heart failure: New insights from continuous monitoring devices. *Current Heart Failure Reports, 6*(4), 287–292.

Akselrod, S., Gordon, D., Ubel, F. A., Shannon, D. C., Berger, A. C., & Cohen, R. J. (1981). Power spectrum analysis of heart rate fluctuation: A quantitative probe of beat-to-beat cardiovascular control. *Science., 213*(4504), 220–222.

Amorim, D. (1981). Is there autonomic impairment in congestive (dilated) cardiomyopathy? *The Lancet., 317*(8219), 525–527.

Au - Hamza SM, Au - Hall JE.. (2018). Novel approach for simultaneous recording of renal sympathetic nerve activity and blood pressure with intravenous infusion in conscious, unrestrained mice. *Journal of Visualized Experiments: Jove, 132*, Article e54120.

Bas, R., Vallverdu, M., Valencia, J. F., Voss, A., de Luna, A. B., & Caminal, P. (2015). Evaluation of acceleration and deceleration cardiac processes using phase-rectified signal averaging in healthy and idiopathic dilated cardiomyopathy subjects. *Medical Engineering & Physics, 37*(2), 195–202.

Bauer, A., Kantelhardt, J. W., Barthel, P., Schneider, R., Makikallio, T., Ulm, K., et al. (2006a). Deceleration capacity of heart rate as a predictor of mortality after myocardial infarction: Cohort study. *Lancet., 367*(9523), 1674–1681.

Bauer, A., Kantelhardt, J. W., Barthel, P., Schneider, R., Mäkikallio, T., Ulm, K., et al. (2006b). Deceleration capacity of heart rate as a predictor of mortality after myocardial infarction: Cohort study. *The Lancet., 367*(9523), 1674–1681.

Benjamin, E. J., Virani, S. S., Callaway, C. W., Chamberlain, A. M., Chang, A. R., Cheng, S., et al. (2018). Heart disease and stroke statistics-2018 update: A report from the American Heart Association. *Circulation., 137*(12), e67–e492.

Binkley, P. F., Nunziata, E., Haas, G. J., Nelson, S. D., & Cody, R. J. (1991). Parasympathetic withdrawal is an integral component of autonomic imbalance in congestive heart failure: Demonstration in human subjects and verification in a paced canine model of ventricular failure. *Journal of the American College of Cardiology, 18*(2), 464–472.

Boehler, C., Carli, S., Fadiga, L., Stieglitz, T., & Asplund, M. (2020). Tutorial: Guidelines for standardized performance tests for electrodes intended for neural interfaces and bioelectronics. *Nature Protocols, 15*(11), 3557–3578.

Bouairi, E., Neff, R., Evans, C., Gold, A., Andresen, M. C., & Mendelowitz, D. (2004). Respiratory sinus arrhythmia in freely moving and anesthetized rats. *Journal of Applied Physiology, 97*(4), 1431–1436.

Byku, M., & Mann, D. L. (2016). Neuromodulation of the failing heart: Lost in translation? *JACC Basic to Translational Science, 1*(3), 95–106.

Charles, C. J., Rademaker, M. T., Scott, N. J. A., & Richards, A. M. (2020). Large animal models of heart failure: Reduced vs. Preserved ejection fraction. *Animals., 10*(10), 1906.

Heart rate variability: Standards of measurement, physiological interpretation and clinical use. Task Force of the European Society of Cardiology and the North American Society of Pacing and Electrophysiology. *Circulation., 93*(5), (1996), 1043–1065.

Cohn, J. N., Levine, T. B., Olivari, M. T., Garberg, V., Lura, D., Francis, G. S., et al. (1984). Plasma norepinephrine as a guide to prognosis in patients with chronic congestive heart failure. *The New England Journal of Medicine., 311*(13), 819–823.

Cole, C. R., Blackstone, E. H., Pashkow, F. J., Snader, C. E., & Lauer, M. S. (1999). Heart-rate recovery immediately after exercise as a predictor of mortality. *The New England Journal of Medicine., 341*(18), 1351–1357.

Coleman, H. N., Taylor, R. R., Pool, P. E., Whipple, G. H., Covell, J. W., Ross, J., et al. (1971). Congestive heart failure following chronic tachycardia. *American Heart Journal, 81*(6), 790–798.
Coumel, P., & Leenhardt, A. (1991). Mental activity, adrenergic modulation, and cardiac arrhythmias in patients with heart disease. *Circulation., 83*(4 Suppl). II58-70.
Dixon, J. A., & Spinale, F. G. (2009). Large animal models of heart failure. *Circulation: Heart Failure, 2*(3), 262–271.
Dunlap, M. E., Kinugawa, T., Sica, D. A., & Thames, M. D. (2019). Cardiopulmonary baroreflex control of renal sympathetic nerve activity is impaired in dogs with left ventricular dysfunction. *Journal of Cardiac Failure, 25*(10), 819–827.
Eckberg, D. L., Drabinsky, M., & Braunwald, E. (1971). Defective cardiac parasympathetic control in patients with heart disease. *The New England Journal of Medicine., 285*(16), 877–883.
Esler, M., Willett, I., Leonard, P., Hasking, G., Johns, J., Little, P., et al. (1984). Plasma noradrenaline kinetics in humans. *Journal of the Autonomic Nervous System, 11*(2), 125–144.
Esler, M., Jennings, G., Korner, P., Willett, I., Dudley, F., Hasking, G., et al. (1988). Assessment of human sympathetic nervous system activity from measurements of norepinephrine turnover. *Hypertension., 11*(1), 3–20.
Florea, V. G., & Cohn, J. N. (2014). The autonomic nervous system and heart failure. *Circulation Research, 114*(11), 1815–1826.
Goldberger, J. J., Arora, R., Buckley, U., & Shivkumar, K. (2019). Autonomic nervous system dysfunction: JACC focus seminar. *Journal of the American College of Cardiology, 73*(10), 1189–1206.
Halliwill, J. R., & Billman, G. E. (1992). Effect of general anesthesia on cardiac vagal tone. *The American Journal of Physiology, 262*(6 Pt 2), H1719–H1724.
Hanna, P., Shivkumar, K., & Ardell, J. L. (2018). Calming the nervous heart: Autonomic therapies in heart failure. *Cardiac Failure Review, 4*(2), 92–98.
Hart, E. C., Head, G. A., Carter, J. R., Wallin, B. G., May, C. N., Hamza, S. M., et al. (2017). Recording sympathetic nerve activity in conscious humans and other mammals: Guidelines and the road to standardization. *American Journal of Physiology. Heart and Circulatory Physiology, 312*(5). H1031-H51.
Hayano, J., & Yuda, E. (2019). Pitfalls of assessment of autonomic function by heart rate variability. *Journal of Physiological Anthropology, 38*(1), 3.
Iellamo, F., Sala-Mercado, J. A., Ichinose, M., Hammond, R. L., Pallante, M., Ichinose, T., et al. (2007). Spontaneous baroreflex control of heart rate during exercise and muscle metaboreflex activation in heart failure. *American Journal of Physiology. Heart and Circulatory Physiology, 293*(3). H1929-H36.
Imai, K., Sato, H., Hori, M., Kusuoka, H., Ozaki, H., Yokoyama, H., et al. (1994). Vagally mediated heart rate recovery after exercise is accelerated in athletes but blunted in patients with chronic heart failure. *Journal of the American College of Cardiology, 24*(6), 1529–1535.
Ishise, H., Asanoi, H., Ishizaka, S., Joho, S., Kameyama, T., Umeno, K., et al. (1998). Time course of sympathovagal imbalance and left ventricular dysfunction in conscious dogs with heart failure. *Journal of Applied Physiology, 84*(4), 1234–1241.
Kaye, D. M., Lefkovits, J., Jennings, G. L., Bergin, P., Broughton, A., & Esler, M. D. (1995). Adverse consequences of high sympathetic nervous activity in the failing human heart. *Journal of the American College of Cardiology, 26*(5), 1257–1263.
Khuanjing, T., Palee, S., Chattipakorn, S. C., & Chattipakorn, N. (2020). The effects of acetylcholinesterase inhibitors on the heart in acute myocardial infarction and heart failure: From cells to patient reports. *Acta Physiologica, 228*(2), Article e13396.
La Rovere, M. T., Pinna, G. D., & Raczak, G. (2008). Baroreflex sensitivity: Measurement and clinical implications. *Annals of Noninvasive Electrocardiology, 13*(2), 191–207.
Lopshire, J. C., & Zipes, D. P. (2014). Spinal cord stimulation for heart failure: preclinical studies to determine optimal stimulation parameters for clinical efficacy. *Journal of Cardiovascular Translational Research, 7*(3), 321–329.
McDonagh, T. A., Metra, M., Adamo, M., Gardner, R. S., Baumbach, A., Böhm, M., et al. (2021). 2021 ESC Guidelines for the diagnosis and treatment of acute and chronic heart failure: Developed by the Task Force for the diagnosis and treatment of acute and chronic heart failure of the European Society of Cardiology (ESC) With the special contribution of the Heart Failure Association (HFA) of the ESC. *European Heart Journal, 42*(36), 3599–3726.
Moe, G. W., & Armstrong, P. (1999). Pacing-induced heart failure: A model to study the mechanism of disease progression and novel therapy in heart failure. *Cardiovascular Research, 42*(3), 591–599.
Mondritzki, T., Boehme, P., White, J., Park, J. W., Hoffmann, J., Vogel, J., et al. (2018). Remote left ventricular hemodynamic monitoring using a novel Intracardiac sensor. *Circulation. Cardiovascular Interventions, 11*(5).
Motte, S., Mathieu, M., Brimioulle, S., Pensis, A., Ray, L., Ketelslegers, J.-M., et al. (2005). Respiratory-related heart rate variability in progressive experimental heart failure. *American Journal of Physiology. Heart and Circulatory Physiology, 289*(4). H1729-H35.
Notarius, C. F., & Floras, J. S. (2001). Limitations of the use of spectral analysis of heart rate variability for the estimation of cardiac sympathetic activity in heart failure. *Europace, 3*(1), 29–38.
Ootaki, C., Manzo, A., Kamohara, K., Popovic, Z. B., Fukamachi, K., & Ootaki, Y. (2008). Heart rate variability in a progressive heart failure model with rapid ventricular pacing. *The Heart Surgery Forum., 11*(5), E295–E299.
Pagani, M., Lombardi, F., Guzzetti, S., Rimoldi, O., Furlan, R., Pizzinelli, P., et al. (1986). Power spectral analysis of heart rate and arterial pressure variabilities as a marker of sympatho-vagal interaction in man and conscious dog. *Circulation Research, 59*(2), 178–193.
Patel, H. C., Rosen, S. D., Lindsay, A., Hayward, C., Lyon, A. R., & di Mario, C. (2013). Targeting the autonomic nervous system: Measuring autonomic function and novel devices for heart failure management. *International Journal of Cardiology, 170*(2), 107–117.
Piccirillo, G., Magrì, D., D'Alessandro, G., Fiorucci, C., Moscucci, F., Di Iorio, C., et al. (2018). Oscillatory behavior of *P* wave duration and *PR* interval in experimental congestive heart failure: A preliminary study. *Physiological Measurement, 39*(3), Article 035010.
Pierpont, G. L., & Voth, E. J. (2004). Assessing autonomic function by analysis of heart rate recovery from exercise in healthy subjects. *The American Journal of Cardiology., 94*(1), 64–68.
Pumprla, J., Howorka, K., Groves, D., Chester, M., & Nolan, J. (2002). Functional assessment of heart rate variability: Physiological basis and practical applications. *International Journal of Cardiology, 84*(1), 1–14.
Recchia, F. A., & Lionetti, V. (2007). Animal models of dilated cardiomyopathy for translational research. *Veterinary Research Communications, 31*(1), 35–41.
Rizas, K. D., Eick, C., Doller, A. J., Hamm, W., von Stuelpnagel, L., Zuern, C. S., et al. (2018). Bedside autonomic risk stratification after myocardial infarction by means of short-term deceleration capacity of heart rate. *Europace, 20*(FI1). f129-f36.
Rizas, K. D., Doller, A. J., Hamm, W., Vdovin, N., von Stuelpnagel, L., Zuern, C. S., et al. (2019). Periodic repolarization dynamics as a risk predictor after myocardial infarction: Prospective validation study. *Heart Rhythm, 16*(8), 1223–1231.
Schwartz, P. J., La Rovere, M. T., De Ferrari, G. M., & Mann, D. L. (2015). Autonomic modulation for the management of patients with chronic heart failure. *Circulation. Heart Failure, 8*(3), 619–628.
Shaffer, F., & Ginsberg, J. P. (2017). An overview of heart rate variability metrics and norms. Front. *Public Health, 5*, 258.
Spannbauer, A., Traxler, D., Zlabinger, K., Gugerell, A., Winkler, J., Mester-Tonczar, J., et al. (2019). Large animal models of heart failure with reduced ejection fraction (HFrEF). *Frontiers in Cardiovascular Medicine.*, 6.
Stieglitz, T. (2020). Of man and mice: Translational research in neurotechnology. *Neuron., 105*(1), 12–15.
Triposkiadis, F., Karayannis, G., Giamouzis, G., Skoularigis, J., Louridas, G., & Butler, J. (2009). The sympathetic nervous system in heart failure physiology, pathophysiology, and clinical implications. *Journal of the American College of Cardiology, 54*(19), 1747–1762.
Tsioufis, C., Iliakis, P., Kasiakogias, A., Konstantinidis, D., Lovic, D., Petras, D., et al. (2017). Non-pharmacological modulation of the autonomic nervous system for heart failure treatment: Where do we stand? *Current Vascular Pharmacology, 16*(1), 30–43.
van Bilsen, M., Patel, H. C., Bauersachs, J., Bohm, M., Borggrefe, M., Brutsaert, D., et al. (2017). The autonomic nervous system as a therapeutic target in heart failure: A scientific position statement from the Translational Research Committee of the Heart Failure Association of the European Society of Cardiology. *European Journal of Heart Failure, 19*(11), 1361–1378.
Vatner, S. F., & Braunwald, E. (1975). Cardiovascular control mechanisms in the conscious state. *The New England Journal of Medicine., 293*(19), 970–976.
Wagner, B. R., & Frishman, W. H. (2018). Devices for autonomic regulation therapy in heart failure with reduced ejection fraction. *Cardiology in Review, 26*(1), 43–49.
Whipple, G. H. (1962). Reversible congestive heart failure due to chronic rapid stimulation of the normal heart. *Proceedings of the New England Cardiovascular Society, 20*, 39–40.
Zhang, Y., Popovic, Z. B., Bibevski, S., Fakhry, I., Sica, D. A., Van Wagoner, D. R., et al. (2009). Chronic vagus nerve stimulation improves autonomic control and attenuates systemic inflammation and heart failure progression in a canine high-rate pacing model. *Circulation. Heart Failure, 2*(6), 692–699.
Zhou, S. X., Lei, J., Fang, C., Zhang, Y. L., & Wang, J. F. (2009). Ventricular electrophysiology in congestive heart failure and its correlation with heart rate variability and baroreflex sensitivity: A canine model study. *Europace, 11*(2), 245–251.
Ziaeian, B., & Fonarow, G. C. (2016). Epidemiology and aetiology of heart failure. *Nature Reviews. Cardiology, 13*(6), 368–378.
Zou, C., Dong, H., Wang, F., Gao, M., Huang, X., Jin, J., et al. (2016). Heart acceleration and deceleration capacities associated with dilated cardiomyopathy. *European Journal of Clinical Investigation, 46*(4), 312–320.
Zucker, I. H., Hackley, J. F., Cornish, K. G., Hiser, B. A., Anderson, N. R., Kieval, R., et al. (2007). Chronic baroreceptor activation enhances survival in dogs with pacing-induced heart failure. *Hypertension., 50*(5), 904–910.